The use of a handheld Terahertz pulsed imaging device to differentiate benign and malignant breast tissue with a view to reducing re-operation rates in breast-conserving surgery – a first-in-human feasibility study

Maarten R. Grootendorst[1,2], Tony Fitzgerald[3*], Aida Santa Olalla[1], Susan Brouwer de Koning[1,2], Alessia Portieri[4], Mieke Van Hemelrijck[1], Matthew R. Young[2], Julie Owen[5], Massi Cariati[1,2], Michael Pepper[4,6], Ton Coolen[7], Vincent Wallace[3], Sarah E. Pinder[5], Arnie Purushotham[1,2]*

**: joined first author*

[1] – King's College London, Division of Cancer Studies, Breast Cancer Surgery Group, London, UK;

[2] – Department of Breast Surgery, Guy's and St Thomas' NHS Foundation Trust, London, UK;

[3] – School of Physics, University of Western Australia, Perth, Australia;

[4] – Teraview Ltd., Cambridge, UK;

[5] – King's College London, Division of Cancer Studies, King's Health Partners Cancer Biobank and Breast Pathology Research Group, London, UK;

[6] – London Centre for Nanotechnology, University College London, UK;

[7] – King's College London, Department of Mathematics, London, UK;

Corresponding author: Professor Arnie Purushotham, Department of Research Oncology, 3rd Floor Bermondsey Wing, Guy's Hospital, SE1 9RT, London. Email: arniepurushotham@gmail.com
Phone: +44 (0) 207 188 3027. Fax: +44 (0) 207 188 0919.

Running title (60 characters): Terahertz pulsed imaging for breast tumour margin assessment

Keywords (5): Terahertz pulsed imaging, breast-conserving surgery, tumour margins, first-in-human, diagnostic accuracy

Category of manuscript: Original paper

Word count: 4010

Surgical relevance (150 words)

There is a clear need for more accurate techniques to assess tumour resection margins intraoperatively in breast-conserving surgery (BCS), as to date 10 – 30% of patients require further surgery to achieve clear margins. Due to the sensitivity of THz radiation to changes in water content and tissue composition, the millimetric penetration depth and submillimeter imaging resolution, Terahertz pulsed imaging (TPI) represents a promising technology for intraoperative margin assessment. A TPI handheld probe system (Teraview, Cambridge, UK) has been developed to facilitate the use of TPI to scan breast specimens *ex vivo*. In this first-in-human study, we found that the TPI probe can discriminate invasive breast cancer from benign breast tissue with a high sensitivity (86%) and an encouraging degree of accuracy (75%). These promising results warrant larger studies to assess the diagnostic accuracy of TPI on different cancer types including DCIS, and its impact on re-operation rate.

Abstract (250 words)

Background:

There is a clear need for developing new techniques to more accurately and adequately assess tumour resection margins during breast-conserving surgery (BCS), as currently approximately 10 – 30% of patients undergoing BCS require a re-operation to achieve clear margins. This first-in-human study evaluates the diagnostic accuracy of terahertz pulsed imaging (TPI) to discriminate benign from malignant breast tissue *ex vivo.*

Method:

A total of 46 freshly excised invasive breast cancer samples from 32 patients were scanned with a TPI handheld probe system (Teraview Ltd., Cambridge, UK). For each sample, detailed pathology was obtained and correlated with the THz data. Two data reduction and classification methods were applied to the THz data to determine diagnostic accuracy: (1) heuristic parameters in combination with support vector machine (SVM) classification, and (2) Gaussian wavelet deconvolution in combination with Bayesian classification.

Results:

On the full dataset accuracy, sensitivity, specificity, positive predictive value and negative predictive value was 75%, 86%, 66%, 67% and 85% for method 1, and 69%, 87%, 54%, 60%, 84% for method 2, respectively. By excluding high percentage fibrous tissue diagnostic performance increased to 88%, 87%, 96%, 98% and 61%, respectively.

Conclusion:

The TPI handheld probe can discriminate invasive breast cancer from benign breast tissue with a high sensitivity and an encouraging degree of accuracy. Accurate discrimination of cancer from tissue containing a high percentage of fibrous cells is challenging. Larger studies are warranted to assess the performance of this technique on different tumour types including DCIS, and its impact on re-operation rate.

Introduction

Breast cancer is by far the most common cancer among women worldwide[1]. A combination of an increased use of screening mammography, and neoadjuvant chemotherapy and endocrine therapy to downstage the size of the tumour, has significantly increased the number of patients suitable for breast-conserving surgery (BCS). Currently approximately two-thirds of newly diagnosed breast cancer patients in the United Kingdom and the United States undergo BCS as initial treatment[2, 3].

A key problem in BCS to date is that approximately 10 – 30% of patients require a re-operation because of close or positive tumour margins on postoperative histopathological analysis[4-6]. A positive margin, defined as no 'tumour on ink', is associated with a 2-fold increased risk for developing local recurrence [7, 8]. What constitutes an adequate negative margin of excision is a subject of intense debate; the 2015 Association of Breast Surgery (ABS) consensus agreement defined a clear histological margin for invasive cancer and ductal carcinoma *in situ* (DCIS) as tumour cells >1 mm from the inked resection edge[9].

Re-operations potentially have a significant impact on patients and healthcare systems. They can result in an increased rate of surgical complications[10], compromise cosmetic outcome[11], delay receipt of adjuvant therapy, and increase anxiety and stress for patients and their families. Re-excision surgery also presents a high cost burden; a recent study in the United States showed that the costs for a re-excision was $4721 per patient[12].

In an attempt to decrease the re-operation rate, techniques to intraoperatively assess tumour resection margins have been developed. The clinically established techniques include specimen radiography, intraoperative ultrasound, radiofrequency spectroscopy, frozen section analysis and touch imprint cytology. However, all these techniques have limitations in terms of diagnostic accuracy, logistical or technical demands, or cost-effectiveness[13]. Emerging techniques include Raman spectroscopy[14], diffuse reflectance spectroscopy[15-19], optical coherence tomography[20-22], mass spectroscopy[23, 24], bio-impedance spectroscopy[25], and (targeted) fluorescence imaging[26]. These techniques also have unique limitations, and their potential value for improving quality of care and reducing health care costs is yet unknown.

Terahertz pulsed imaging (TPI) employs terahertz radiation (0.1 – 10 THz) for imaging biological tissue. Due to the millimetric penetration depth and sensitivity of THz radiation to changes in water content and tissue composition, and the submillimeter imaging resolution of TPI, this technique holds

promise for imaging cancer[27]. Work performed to date has shown the ability of TPI to discriminate malignant from benign tissue of skin, colon, oral, gastric, brain and breast cancer[28]. In 2006, Fitzgerald *et al.* were the first to demonstrate the potential of TPI for identifying breast cancer during BCS[29]. They measured a total of 22 freshly excised breast tissue samples, and demonstrated a good correlation in tumour size and shape between TPI and histopathology. To better understand the origin of the observed contrast on TPI, Ashworth *et al.* used THz spectroscopy and showed that the optical properties (i.e. absorption coefficient and refractive index) of tumour were different to that of normal breast tissue in the THz region of the spectrum[30]. Following from their initial work, Fitzgerald *et al.* imaged 51 breast samples and assessed the diagnostic accuracy of TPI by using a range of THz image parameters and classification techniques[31]. They demonstrated an accuracy, sensitivity and specificity of 91.9%, 90.3% and 92.1%, respectively. However, the TPI device used in their study is not suitable for intraoperative assessment of intact breast specimens due to the requirement for physical tissue disruption to obtain samples that fit the 20 x 20 mm sample holder. Importantly, the tissue samples included in their dataset had a 'homogeneous' tissue composition, i.e. contained more than 50% of a single tissue type. This is not an accurate representation of the tissue composition found at the resection border of patients with close or positive margins, as involved margins are often identified microscopically as a small number of tumour cells immersed in a 'background' of fibrous and/or adipose tissue[32]. Thus, the diagnostic accuracy of TPI for detecting tumour close or at the margin remains underdetermined.

To facilitate the use of TPI to scan tumour resection margins intraoperatively, Teraview Ltd. (Cambridge, UK) has developed a handheld probe system. A first-in-human, single centre study was performed to evaluate the ability of the TPI handheld probe to discriminate benign from malignant breast tissue in an *ex vivo* setting. The aims of the study were to obtain a dataset that closely resembles the mixture of benign and tumour tissue commonly found at the resection border of patients with involved margins, and to evaluate the diagnostic performance of the TPI handheld probe in terms of accuracy, sensitivity, specificity and predictive values using two data analysis and classification methods.

Methods

TPI handheld probe system

The TPI handheld probe produces and detects THz pulses by guiding laser pulses from a Ti:Sapphire laser (Menlo Systems GmbH, Martinsreid, Germany) down optical fibres to a GaAs photoconductive emitter and detector (Supplementary Material Figure 1**)**. The 0.1 – 1.8 THz pulses are then guided by an oscillating mirror onto a quartz window present at the tip of the probe, scanning 26 pixels in an area of 15 x 2 mm at a frequency of 4 Hz (Supplementary Material Figure 2). During scanning each pixel acquires THz pulses over time to form a TPI image (Figure 1).

Data acquisition

Between August 2013 and August 2014, breast tissue samples from patients who underwent BCS or mastectomy at Guy's Hospital in London were scanned with the TPI probe after written informed consent was obtained (REC 12-EE-0493). Within 60 minutes post-excision, BCS and mastectomy specimens were inked and sliced by an Advanced Practitioner in the King's Health Partners Cancer Biobank located adjacent to the operating theatre. Uninked tissue samples were obtained for the study subject to the amount of tissue required for diagnostic purposes.

Prior to scanning the samples, a Tegaderm layer (3M Tegaderm Film, 3M, Bracknell, UK) was applied to the probe's quartz window, and the remainder of the probe was wrapped in a disposable protective sheath to prevent contamination from tissue. A 60 second water measurement was performed to assess the signal intensity and shape of the THz pulses emitted by the TPI system on each day of measurement. To enable consistent and controlled TPI measurements, tissue samples were placed in a standard histology cassette (Unisette^{TM}, Simport, Beloeil, Canada) that tightly fitted the head of the probe (Supplementary Material Figure 3). All samples were scanned for 20 seconds. Upon completion of each measurement a photograph of the sample in the cassette was taken to facilitate accurate correlation of the TPI data with the final histology slide.

After the sample was scanned, the Tegaderm layer was removed from the probe and a 60 second air measurement was performed that was used as a reference for data processing. For orientation purposes the top and the right surface of the sample were inked red and black respectively, after which the histology cassette containing the sample was closed, and placed in formalin for 24-48 hours, processed, and paraffin wax embedded. Three to 4 micron sections were then cut and stained with haematoxylin and eosin. The histology slides were digitalised, and subsequently analysed using histopathology slide viewer software (NDP.view2, Hamamatsu, UK).

TPI data processing

Each pixel of the TPI probe acquired raw THz pulses throughout the duration of the measurement. These pulses were deconvolved with the reference ("air without Tegaderm") pulses and a double Gaussian filter was applied to reduce noise. All pulses were aligned in time to compensate for small offsets in the phase of the detected pulses due to changes in the optical path length that occur when optical fibres deform slightly with movement during scanning. The deconvolved pulses – called impulse functions - of each pixel were then averaged over time, resulting in 26 impulse functions, one for each of the 26 pixels to be used for discriminating benign from malignant breast tissue (Figure 1).

Correlation of TPI with histopathology

By using the photograph depicting the imprint of the probe's scan window on the sample, and the clear contrast from the air-tissue interface and tissue composition on the TPI image, the 15 x 2 mm TPI scan area was mapped onto the digital histopathology image (Figure 1). To reduce potential inaccuracies in correlating TPI with histopathology, samples were excluded from further analysis if the number of tissue-containing pixels on TPI and histopathology differed by more than three.

Histopathological analysis and selection of TPI data

The digital histopathology slide of each sample was analysed in the viewer software by a specialist experienced breast histopathologist (S.E.P.) for the percentage tissue types of tumour, fibrous, and adipose, respectively. Tissue percentages were reported in 5% intervals. For a subset of samples an inter-rater variability analysis was performed to assess the ability of the histopathologist to consistently score the tissue samples. For this analysis, a total of 92 pixels from 7 tumour samples and 125 pixels from 7 benign samples were re-evaluated in a blinded method by the same histopathologist 8 weeks after the first analysis. Weighted kappa coefficients were calculated to assess the agreement in subgroup classification between evaluation 1 and 2 (*kappa 2* function of the 'irr' package v0.84, R statistical software v3.2.2). A kappa coefficient (κ) greater than 0.80 was considered excellent agreement[33]. A Wilcoxon signed-rank test was performed to assess whether evaluation 1 was statistically significantly different from evaluation 2. The level of significance was defined as $p < 0.05$.

Based on the histopathological information, pixels were selected by drawing region of interests (ROIs) on the TPI images, and subsequently grouped according to tissue type and tissue percentage (Table 1). Pixels containing tumour tissue, and pixels containing pure fibrous tissue or a mixture of fibrous and adipose tissue, were divided into groups of 20% (i.e. 1 – 20%, 21 – 40%, 41 – 60%, 61 – 80%, and 81 – 100%). Pure adipose pixels were grouped separately in a “100% adipose” group.

TPI data analysis and classification

Classification of each of the selected impulse functions as malignant or benign was performed using two data analysis and classification methods: (1) heuristic parameters in combination with SVM classification and (2) Gaussian wavelet deconvolution with Bayesian classification.

The impulse function of each pixel is made of values at 301 time points, and given that information from both the time and frequency domain can be used to classify pixels, it was advantageous to reduce the dimensionality of the data for classification. This was done by using parameters that described significant features in the impulse function or spectrum. Since a large number of time points or frequency points can be selected to form a parameter, a Receiver operator Characteristics (ROC) analysis was used to select the optimal characterising parameters. The area under the ROC curve (AUROC) was used as an estimate of the classification ability of each parameter (illustrated in Supplementary Material Figure 4). AUROC analysis was done on the data from 3 pathology groups; (i) the full tumour and fibrous groups (excluding pure adipose), (ii) the tumour and 100% fibrous groups, and (iii) the tumour and 100% adipose groups. From this analysis the top 11 parameters were selected to be used for classification of the data in the support vector machine (SVM) (Table 2). To avoid effects of overfitting, the parameters chosen were tested to ensure they were not correlated, eliminating any parameters with an absolute correlation coefficient of 0.7 or more. The SVM function used for classification was from the Matlab native functions *svmtrain.m* and *svmclassify.m* using a radial basis function as the kernel to form the decision boundaries (MATLAB 2013A, The Mathworks Inc., Natick, MA, 2013). A grid search method was applied to optimise the sigma and box constraint terms as 0.3 and 1.1, respectively.

Tissue classification was also performed using Gaussian wavelet deconvolution in combination with a Bayesian classifier. In contrast to heuristic parameters, Gaussian wavelet deconvolution can be applied to the full impulse function. This method was considered a suitable approach because of the

similarities between the signal features of a Gaussian function and its derivatives, and the TPI impulse functions from breast tissue. Gaussian derivatives of order 0 (normal Gaussian function), 1, 2, 3 and 4 were applied to the impulse function of each pixel. Higher order Gaussian derivatives were not used to avoid potential overfitting. The Gaussian deconvolved data were then fed into a Bayesian classification algorithm[34], and classified as tumour, fibrous or adipose, respectively. Adipose and fibrous tissue were then grouped together as 'benign' in order to calculate the diagnostic performance of TPI. Similar to SVM, pixels were marked as tumour when containing any amount of cancer cells. Wavelet deconvolution and Bayesian classification was performed using the *MCLUST* package in R statistical software[35].

The SVM and Bayesian classifier were trained individually using the leave one out method (LOO), leaving out the pixels of a single sample to be classified, and training each classifier on the other samples. The trained classifiers were then applied to the pixels of the sample that was left out. This process was repeated for all the samples, leaving each of them out in turn, and the results compiled to give accuracy, sensitivity, specificity, positive predictive value, and negative predictive value for distinguishing malignant from benign tissue.

Results

Tissue sample characteristics and histopathology inter-rater reliability

In total, 126 samples from 106 patients were scanned; 46 samples from 32 patients met the strict criteria established to ensure accurate correlation of TPI with histology, i.e. a photograph was available of the sample in the histology cassette, and the number of tissue containing pixels on TPI and histopathology differed by 3 or less. These samples were included for analysis. Of these, 20 samples contained tumour; 16 invasive ductal/no special type (NST) carcinoma, 2 NST admixed with DCIS, 2 invasive lobular carcinoma (ILC). Twenty-two samples contained pure fibrous tissue or a mixture of fibrous and adipose tissue, and 4 samples contained pure adipose tissue. The total number of pixels for analysis was 257; the breakdown in terms of tissue composition is given in Table 1.

The inter-rater reliability analysis showed excellent agreement in cell density subgroup classification between histopathological evaluation 1 and evaluation 2 ($\kappa = 0.89$) ($p = NS$). This confirmed that the established subgroups reliably reflected the tissue composition of the samples, and

thus could be used to evaluate the performance of the TPI handheld probe system for different tissue groups.

Heuristic parameters and SVM classification

A total of 11 parameters were selected based on the AUROC analysis: 10 time domain parameters and 1 frequency parameter (Table 2) (Supplementary Material Figure 5). Most of the time domain parameters capture the area around the minimum amplitude of the pulse, and the return to baseline after the minimum. P1 – P7 were selected based on their overall ability of discriminating tumour from fibrous tissue with adipose, while P8 – P11 were specifically selected to enhance the TPI probe's ability to discriminate tumour from pure fibrous tissue. All 11 parameters showed strong discriminative power to distinguish tumour from pure adipose tissue (mean AUROC = 0.97, range 0.84 – 1.0).

The SVM classification results of the individual parameters, and the combination of parameters that performed best in terms of accuracy, may be found in Table 3. Overall the combination of P1 and P6 provided the best performance with an accuracy, sensitivity, specificity, positive predictive value (PPV) and negative predictive value (NPV) of 75%, 86%, 66%, 67% and 85%, respectively. These values were obtained as a result of 16 of the 115 tumour pixels being misclassified as benign; 48 of the 142 benign pixels were misclassified as tumour. All misclassified tumour pixels had a tumour content ≤60%. Of the 48 misclassified benign pixels, 46 were fibrous pixels containing 81 – 100% fibrous cells; only 2 of the 1 – 80% fibrous pixels were misclassified as tumour, and all 26 pure adipose pixels were correctly identified as benign. The two-dimensional parametric plot of P1 and P6 showed very little differences between tumour and high percentage fibrous tissue (Figure 2A); this provides an explanation for why most of the SVM classification errors occurred in these two tissue groups (Figure 2B). Pixels with a high adipose content (1 – 80% fibrous pixels and pure adipose pixels) were generally clearly different from pixels containing a high percentage of fibrous tissue (81 – 100%) and cancer (Figure 2A). The accuracy, sensitivity, specificity, PPV and NPV for discriminating 1 – 80% fibrous and pure adipose tissue from tumour (i.e. excluding the predominantly fibrous group with 81 – 100% purity) was 87%, 86%, 96%, 98%, 59%, respectively.

Gaussian wavelet deconvolution and Bayesian classification

The accuracy, sensitivity, specificity, PPV and NPV of Gaussian wavelet deconvolution and Bayesian classification was 69%, 87%, 54%, 60%, 84%, respectively (Table 3). Of the 115 tumour pixels, 15

were misclassified as benign. All misclassified pixels contained ≤60% tumour cells. Sixty-six of the 142 benign pixels were wrongly classified as tumour; 64 of these were 81 – 100% fibrous pixels, only two 1 – 80% fibrous pixels were misclassified. All pure adipose pixels were correctly classified. The accuracy, sensitivity, specificity, PPV and NPV of the handheld probe for discriminating 1 – 80% fibrous and pure adipose from tumour was 88%, 87%, 96%, 98% and 61%, respectively.

Discussion

This first-in-human study has evaluated the performance of a TPI handheld probe system to discriminate breast cancer from benign breast tissue in an *ex vivo* setting. A total of 257 pixels acquired from scanning 46 breast tissue samples were included for analysis. The tumour samples predominantly contained low-to-moderate tumour cell percentages, resembling the tissue composition found at the resection border of breast specimens from patients with positive margins after BCS. Two data analysis and classification methods were assessed: (1) heuristic parameters in combination with SVM classification and (2) Gaussian wavelet deconvolution with Bayesian classification. On the full dataset the former provided the best performance in terms of accuracy (75%). Both methods had excellent sensitivity (86% and 87%, respectively) and thus show promise for identifying tumour cells close or at the resection margins, allowing immediate further excision of appropriate margins and reducing subsequent second operations/re-excision rates if the TPI handheld probe had been used intraoperatively. Specificity was 66% and 54% for SVM and Bayesian respectively; for both methods the lower specificity was due to pixels with 81 – 100% fibrous tissue that were wrongly classified as tumour. The accuracy, sensitivity and specificity increased to 88%, 87%, and 96% respectively after excluding the 81 – 100% fibrous tissue from the classification results.

The reported pooled sensitivity and specificity of the established techniques to intraoperatively assess tumour margins during BCS are 53% (95% CI 45 – 61%) and 84% (95% CI 77 – 89%) for specimen radiography, 59% (95% CI 36 – 79%) and 81% (95% CI 66 – 91%) for ultrasound imaging, 71.4% and 67.7% for radiofrequency spectroscopy, 86% (95% CI 78 – 91%) and 96% (95% CI 92 – 98%) for frozen section analysis, and 91% (95% IC 71 – 97%) and 95% (95% IC 90 – 98%) for imprint cytology, respectively[13]. Thus, based on the results of the present study, the TPI handheld probe appears to perform similarly or better in terms of sensitivity, while the performance in terms of specificity is lower. Compared to specimen radiography and ultrasound, which are also imaging technologies, TPI

has the potential advantage that image interpretation is not needed as the device can provide a binary read-out (tumour or no tumour). This may overcome the need for the extensive training required for obtaining ultrasound accreditation[36]. Potential advantages over the histopathological techniques frozen section analysis and imprint cytology are the fact that TPI is non-invasive (i.e. physical tissue disruption is not required), does not require an on-site cytologist or histopathologist, and allows for assessing a larger tissue surface.

Results published to date on the diagnostic performance of emerging techniques for margin assessment have shown a sensitivity and specificity of 92% (95% CI 86 – 96%) and 97% (95% CI 93 – 98%) for Raman spectroscopy[14],, 67 – 85% and 67 – 96% for diffuse reflectance spectroscopy[15-19], 60 – 100% and 69 – 92% for optical coherence tomography[20-22], 93 – 100% and 91.9 – 100% for mass spectroscopy[23, 24], and 87% and 76% for bioimpedance spectroscopy[25], respectively. Although the performance of the handheld probe in this first-in-human study is somewhat lower than some of the other emerging techniques, TPI uses a different region of the electromagnetic spectrum and thus provides complementary information. It is possible that combinations of technologies could significantly improve the overall accuracy of identifying involved margins.

Several papers have reported on the ability of TPI to discriminate freshly excised benign from malignant breast tissue[29, 31, 37, 38]. Ashworth *et al*. performed a small pilot study using a prototype version of the TPI handheld system[37]; all other studies were conducted with systems not suited for intraoperative imaging of WLE specimens. Similar to our results Ashworth *et al.* found that THz impulse functions from fibrous tissue and breast cancer had strong similarities, while impulse functions from adipose tissue had clearly different features. However, none of the TPI studies in breast cancer published to date have used a dataset representative of the tissue composition found at the resection border of patients with positive margins, as all tumour samples included for analysis contained >50% tumour cells. Thus, the results in our study are the first that can be used to derive insight in the potential benefits of TPI in enabling more accurate and complete tumour resection in BCS.

The accuracy, sensitivity and specificity of the TPI probe for discriminating tumour from mixed fibrous and adipose tissue, and pure adipose tissue, was 87%, 86%, and 96% for SVM, and 88%, 87% and 96% for Bayesian, respectively. Discrimination of these tissue types is most relevant clinically, as the incidence of breast cancer in the UK is highest in older women, who are likely to have fatty or mixed

fibrous and fatty breasts compared to younger women who may have more dense breasts primarily composed of fibrous tissue[39].

While the results of this feasibility study are promising, two limitations were noted. Firstly, the 0.6 mm pixel distance used for correlating TPI and histopathology was based on a linear movement of the THz pulse beam across the 15 x 2 mm scan area. However, in practice the THz beam moves faster in the centre of the scan window and slows down upon reaching the top and bottom boundary, resulting in a larger distance between pixels located in the centre compared to the edges. This introduces a degree of inaccuracy, which was not accounted for in this study. Secondly, the current dataset does not contain THz pulses from cases of pure DCIS. These samples could not be assessed, as DCIS is generally non-palpable and particularly problematic to sample in the fresh state without impairment of gold-standard histological assessment (including the search for foci of invasive disease) However, since DCIS is often the cause of the clinical recommendation for re-operations in BCS, it is of key importance to assess the sensitivity of the TPI handheld probe for detecting DCIS. Based on the results of this feasibility study, a study will be performed at Guy's Hospital in which TPI data will be acquired from the cut surface of incised mastectomy specimens and from intact and incised BCS specimens. By performing a DCIS subgroup analysis, insight should be obtained on the ability of TPI to accurately detect DCIS.

In conclusion, the results of this first-in-human study show that the TPI handheld probe can discriminate invasive breast cancer from benign breast tissue with a high sensitivity and an encouraging degree of accuracy. The main challenge for TPI is accurate discrimination of cancer from tissue containing a high percentage of fibrous cells due to the similarities in the THz pulse between these two types of tissue. Larger studies are warranted to assess the performance of this technique on different tumour types including DCIS, and its impact on re-operation rate.

Disclosures

The authors have no conflicts of interest to disclose.

This study was supported by funding from Guy's and St Thomas' Charity and the Academy of Medical Sciences

Acknowledgments

The authors gratefully acknowledge the excellent support from the King's Health Partners Cancer Biobank, Breast Cancer NOW and the breast care team at Guy's Hospital for their help with patient recruitment. In particular we thank Patrycja Gazinska for digitally scanning the histopathology slides.

References

1. Ferlay J., Soerjomataram I., Ervik M., Dikshit R., Eser S., Mathers C.*, et al.* GLOBOCAN 2012 v1.0, Cancer Incidence and Mortality Worldwide: IARC CancerBase No. 11. In: International Agency for Research on Cancer. World Health Organisation; 2012.

2. Jeevan R, Browne J, Van der Meulen J, Pereira J, Caddy C, Sheppard C*, et al.* First Annual Report of the National Mastectomy and Breast Reconstruction Audit 2008; 2008.

3. McGuire KP, Santillan AA, Kaur P, Meade T, Parbhoo J, Mathias M*, et al.* Are mastectomies on the rise? A 13-year trend analysis of the selection of mastectomy versus breast conservation therapy in 5865 patients. *Ann Surg Oncol* 2009;**16**(10): 2682-90.

4. Jeevan R, Cromwell DA, Trivella M, Lawrence G, Kearins O, Pereira J*, et al.* Reoperation rates after breast conserving surgery for breast cancer among women in England: retrospective study of hospital episode statistics. *BMJ* 2012;**345**: e4505.

5. van der Heiden-van der Loo M, de Munck L, Visser O, Westenend PJ, van Dalen T, Menke MB*, et al.* Variation between hospitals in surgical margins after first breast-conserving surgery in the Netherlands. *Breast Cancer Res Treat* 2012;**131**(2): 691-8.

6. McCahill LE, Single RM, Aiello Bowles EJ, Feigelson HS, James TA, Barney T*, et al.* Variability in reexcision following breast conservation surgery. *JAMA* 2012;**307**(5): 467-75.

7. Houssami N, Macaskill P, Marinovich ML, Morrow M. The association of surgical margins and local recurrence in women with early-stage invasive breast cancer treated with breast-conserving therapy: a meta-analysis. *Ann Surg Oncol* 2014;**21**(3): 717-30.

8. Dunne C, Burke JP, Morrow M, Kell MR. Effect of margin status on local recurrence after breast conservation and radiation therapy for ductal carcinoma in situ. *J Clin Oncol* 2009;**27**(10): 1615-20.

9. Consensus on margins in breast conservation. In: Association of Breast Surgery Annual Conference; 2015; Bournemouth: Association of Breast Surgery (ABS); 2015.

10. Xue DQ, Qian C, Yang L, Wang XF. Risk factors for surgical site infections after breast surgery: a systematic review and meta-analysis. *Eur J Surg Oncol* 2012;**38**(5): 375-81.

11. Heil J, Breitkreuz K, Golatta M, Czink E, Dahlkamp J, Rom J*, et al.* Do reexcisions impair aesthetic outcome in breast conservation surgery? Exploratory analysis of a prospective cohort study. *Ann Surg Oncol* 2012;**19**(2): 541-7.

12. Arora D, Hasan S, Male E, Abid R, Ord C, Dauway E*, et al.* Cost analysis of re-excisions for breast conserving surgery in Central Texas. In: ASCO Annual Meeting; 2015; 2015.

13. St John ER, Al-Khudairi R, Ashrafian H, Athanasiou T, Takats Z, Hadjiminas DJ*, et al.* Diagnostic Accuracy of Intraoperative Techniques for Margin Assessment in Breast Cancer Surgery: A Meta-analysis. *Ann Surg* 2016.

14. Deng K, Zhu C, Ma X, Jia H, Wei Z, Xiao Y*, et al.* Rapid Discrimination of Malignant Breast Lesions from Normal Tissues Utilizing Raman Spectroscopy System: A Systematic Review and Meta-Analysis of In Vitro Studies. *PLoS One* 2016;**11**(7): e0159860.

15. Brown JQ, Bydlon TM, Kennedy SA, Caldwell ML, Gallagher JE, Junker M*, et al.* Optical spectral surveillance of breast tissue landscapes for detection of residual disease in breast tumor margins. *PLoS ONE [Electronic Resource]* 2013;**8**(7): e69906.

16. Wilke LG, Brown JQ, Bydlon TM, Kennedy SA, Richards LM, Junker MK*, et al.* Rapid noninvasive optical imaging of tissue composition in breast tumor margins. *Am J Surg* 2009;**198**(4): 566-74.

17. Keller MD, Majumder SK, Kelley MC, Meszoely IM, Boulos FI, Olivares GM*, et al.* Autofluorescence and diffuse reflectance spectroscopy and spectral imaging for breast surgical margin analysis. *Lasers Surg Med* 2010;**42**(1): 15-23.

18. Laughney AM, Krishnaswamy V, Rizzo EJ, Schwab MC, Barth RJ, Jr., Cuccia DJ*, et al.* Spectral discrimination of breast pathologies in situ using spatial frequency domain imaging. *Breast Cancer Research* 2013;**15**(4): R61.

19. Bigio IJ, Bown SG, Briggs G, Kelley C, Lakhani S, Pickard D*, et al.* Diagnosis of breast cancer using elastic-scattering spectroscopy: preliminary clinical results. *J Biomed Opt* 2000;**5**(2): 221-8.

20. Zysk AM, Chen K, Gabrielson E, Tafra L, May Gonzalez EA, Canner JK*, et al.* Intraoperative Assessment of Final Margins with a Handheld Optical Imaging Probe During Breast-Conserving Surgery May Reduce the Reoperation Rate: Results of a Multicenter Study. *Ann Surg Oncol* 2015;**22**(10): 3356-62.

21. Nguyen FT, Zysk AM, Chaney EJ, Kotynek JG, Oliphant UJ, Bellafiore FJ*, et al.* Intraoperative Evaluation of Breast Tumor Margins with Optical Coherence Tomography. *Cancer Research* 2009;**69**(22): 8790-96.

22. Erickson-Bhatt SJ, Nolan RM, Shemonski ND, Adie SG, Putney J, Darga D*, et al.* Real-time Imaging of the Resection Bed Using a Handheld Probe to Reduce Incidence of Microscopic Positive Margins in Cancer Surgery. *Cancer Res* 2015;**75**(18): 3706-12.

23. Balog J, Sasi-Szabó L, Kinross J, Lewis MR, Muirhead LJ, Veselkov K*, et al.* Intraoperative Tissue Identification Using Rapid Evaporative Ionization Mass Spectrometry. *Science Translational Medicine* 2013;**5**(194): 194ra93.

24. St John ER, Al-Khudairi R, Balog J, Rossi M, Gildea L, Speller A*, et al.* Rapid evaporative ionisation mass spectrometry towards real time intraoperative oncological margin status determination in breast conserving surgery. In: 38th Annual San Antonio Breast Cancer Symposium. San Antonio; 2016.

25. Dixon JM, Renshaw L, Young O, Kulkarni D, Saleem T, Sarfaty M*, et al.* Intra-operative assessment of excised breast tumour margins using ClearEdge imaging device. *European Journal of Surgical Oncology (EJSO)*.

26. Vahrmeijer AL, Hutteman M, van der Vorst JR, van de Velde CJ, Frangioni JV. Image-guided cancer surgery using near-infrared fluorescence. *Nat Rev Clin Oncol* 2013;**10**(9): 507-18.

27. Yu C, Fan S, Sun Y, Pickwell-Macpherson E. The potential of terahertz imaging for cancer diagnosis: A review of investigations to date. *Quant Imaging Med Surg* 2012;**2**(1): 33-45.

28. Fan S, He Y, Ung BS, Pickwell-MacPherson E. The growth of biomedical terahertz research. *Journal of Physics D: Applied Physics* 2014;**47**(37).

29. Fitzgerald AJ, Wallace VP, Jimenez-Linan M, Bobrow L, Pye RJ, Purushotham AD*, et al.* Terahertz pulsed imaging of human breast tumors. *Radiology* 2006;**239**(2): 533-40.

30. Ashworth PC, Pickwell-MacPherson E, Provenzano E, Pinder SE, Purushotham AD, Pepper M*, et al.* Terahertz pulsed spectroscopy of freshly excised human breast cancer. *Opt Express* 2009;**17**(15): 12444-54.

31. Fitzgerald AJ, Pinder S, Purushotham AD, O'Kelly P, Ashworth PC, Wallace VP. Classification of terahertz-pulsed imaging data from excised breast tissue. *J Biomed Opt* 2012;**17**(1): 016005.

32. Park CC, Mitsumori M, Nixon A, Recht A, Connolly J, Gelman R*, et al.* Outcome at 8 years after breast-conserving surgery and radiation therapy for invasive breast cancer: influence of margin status and systemic therapy on local recurrence. *J Clin Oncol* 2000;**18**(8): 1668-75.

33. Khan KS, Chien PF. Evaluation of a clinical test. I: assessment of reliability. *BJOG* 2001;**108**(6): 562-7.

34. Shalabi A, Inoue M, Watkins J, De Rinaldis E, Coolen AC. Bayesian clinical classification from high-dimensional data: Signatures versus variability. *Stat Methods Med Res* 2016.

35. Fraley C, Raftery EA. MCLUST: Software for Model-Based Cluster Analysis. *Journal of Classification* 1999;**16**(2): 297-306.

36. Ahmed M, Rubio IT, Klaase JM, Douek M. Surgical treatment of nonpalpable primary invasive and in situ breast cancer. *Nat Rev Clin Oncol* 2015;**12**(11): 645-63.

37. Ashworth PC, O'Kelly P, Purushotham AD, Pinder SE, Kontos M, Pepper M*, et al.* An intra-operative THz probe for use during the surgical removal of breast tumors. In: Infrared, Millimeter and Terahertz Waves, 2008 IRMMW-THz 2008 33rd International Conference on; 2008 15-19 Sept. 2008; 2008. p. 1-3.

38. Truong BC, Tuan HD, Fitzgerald AJ, Wallace VP, Nguyen HT. A dielectric model of human breast tissue in terahertz regime. *IEEE Trans Biomed Eng* 2015;**62**(2): 699-707.

39. Stomper PC, D'Souza DJ, DiNitto PA, Arredondo MA. Analysis of parenchymal density on mammograms in 1353 women 25-79 years old. *AJR Am J Roentgenol* 1996;**167**(5): 1261-5.

Figures with legends

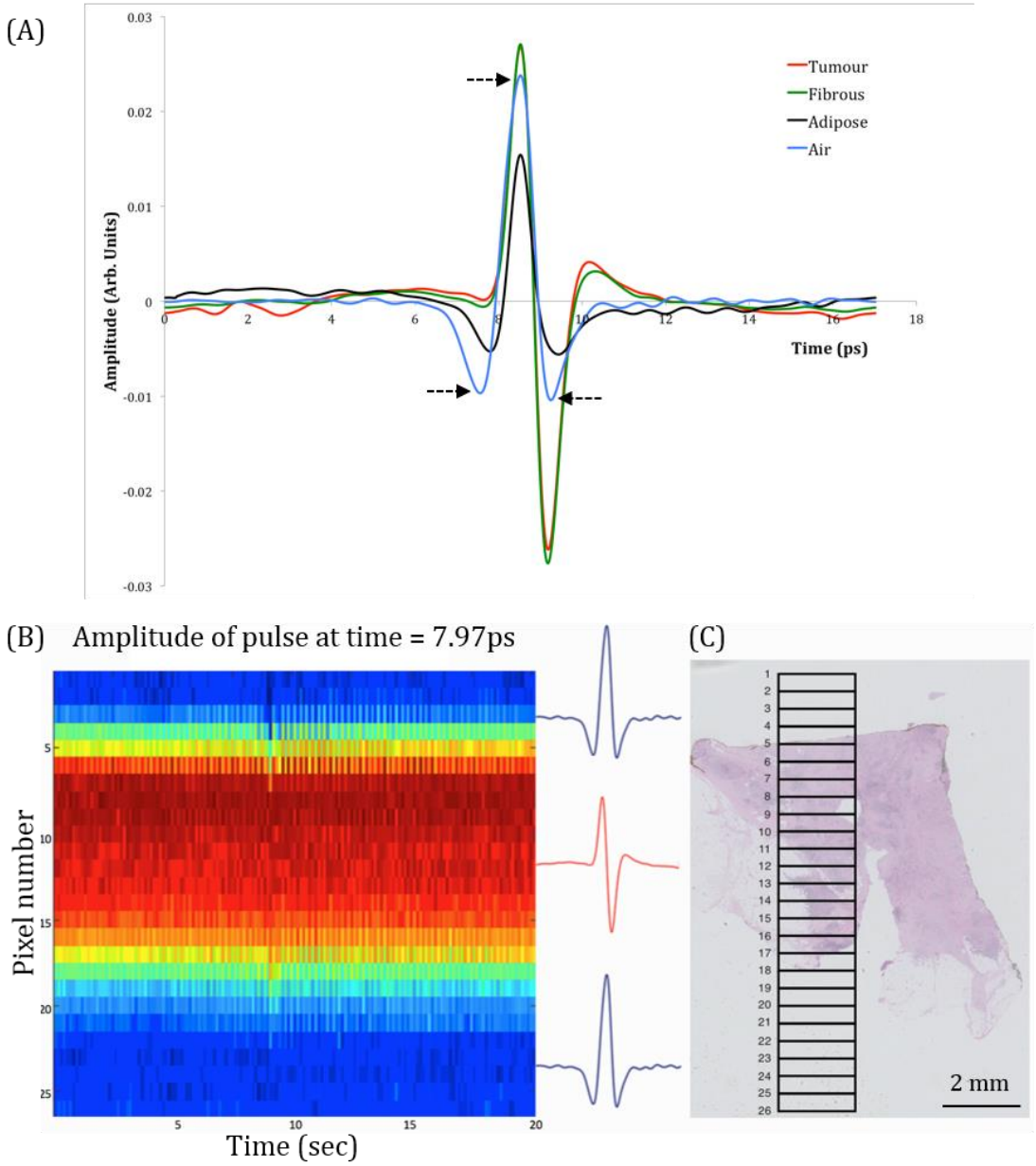

Figure 1: Correlating TPI with histopathology. (A) Typical impulse function of highly tumour, fibrous, and adipose tissue, and air, respectively. Clear differences are seen between the impulse functions from air and from tissue, and between adipose and tumour/fibrous tissue, especially at time points t = 7.97 ps, t = 8.93 ps, and t = 9.67 ps (black arrows). (B) TPI image from sample based on the amplitude of the impulse function at t = 7.97ps. A clear contrast can be seen at the air-tissue interface at pixel 5 and pixel 17. Note an 'edge effect' at these interfaces, causing a distortion in the impulse functions of these pixels. (C) Digital histopathology slide of the same tissue sample. By using the photograph of the sample in combination with the air-tissue interface visible in the TPI image, the TPI 15 x 2 mm scan area can be accurately mapped onto the histopathology slide (black rectangle). The pixels are displayed as intermittent horizontal lines at 0.6 mm distance in the scan window. Pixel 5 – 17 contain invasive ductal/no special type (NST) carcinoma; the percentage of tumour cells in each pixel area ranges between 5 – 10%. The tissue immedialtely surrounding the tumour cells (called background) is composed of fibrous tissue, whilst fatty adipose tissue is seen inferiorly.

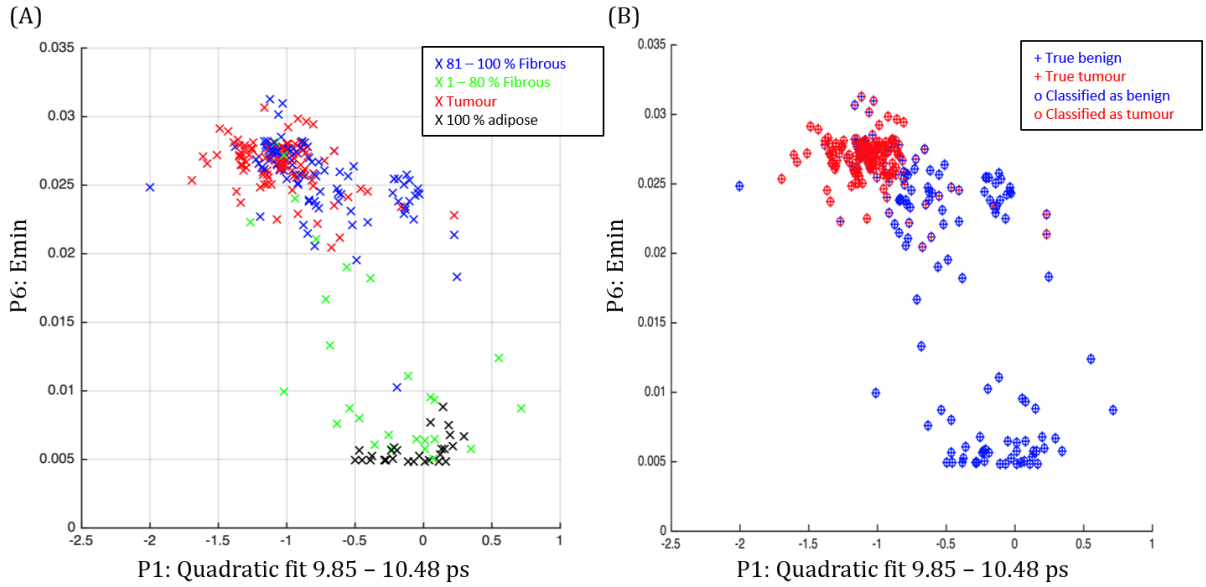

Figure 2: Two-dimensional parametric plot (A) and SVM classification results (B) for the combination of parameters P1 and P6 that performed best in terms of accuracy.

Tables with legends

Table 1: Pixel characteristics analysis dataset. A total of 257 pixels were included in the TPI dataset: 115 tumour pixels, 116 fibrous pixels and 26 pure adipose pixels. The tumour pixels predominantly consisted of invasive ductal/no special type carcinoma (N = 92) and invasive lobular carcinoma (N = 19). Most of the tumour pixels contained a low to moderate percentage of tumour cells ranging between 1 – 60% (N = 98). Almost all tumour cells had a background of pure fibrous tissue; only 5 had a background containing a mix of fibrous and adipose. Most of the fibrous pixels had a high percentage of fibrous cells ranging between 81 – 100% (N = 91). Only 26 of the 257 pixels consisted of pure adipose tissue.

	Tumour					**Fibrous**		**Adipose**
Tissue percentage groups (%)	NST	NST + DCIS	ILC	No. of pixels	BG	No. of pixels	BG	No. of pixels
81 – 100	3	1		4	F	91	A	26[1]
61 – 80	11	2		13	F	2	A	
41 – 60	22		6	28	F	7	A	
21 – 40	33	1	12	46	F: 43 F/A: 3	3	A	
1 – 20	23		1	24	F: 22 F/A: 2	13	A	
No. of pixels	92	4	19	115		116		26

NST = invasive ductal/no special type carcinoma; DCIS = ductal carcinoma *in situ*; ILC = invasive lobular carcinoma; BG = background tissue. In our dataset the background consisted of fibrous tissue (F), adipose tissue (A), or a mixture of fibrous and adipose tissue (F/A).

1. These pixels contained 100% adipose tissue.

Table 2: Overview of selected time domain and frequency domain parameters and their AUROC values.

Parameter	**Definition**	**AUROC value (cell density group)[1]**
P1	*Quadratic fit 9.85 – 10.48 ps*	*0.76 (All T and F)*
P2	*Linear fit 9.42 – 9.67 ps*	*0.73 (All T and F)*
P3	*Amplitude at t = 9.42 ps*	*0.72 (All T and F)*
P4	*Integral 9.14 – 9.65 ps*	*0.72 (All T and F)*
P5	*Peak to peak (Emax minus Emin)*	*0.71 (All T and F)*
P6	*Emin (minimum amplitude)*	*0.70 (All T and F)*
P7	*Amplitude at t = 10.05 ps*	*0.70 (All T and F)*
P8	*Quadratic fit 8.26 – 8.79 ps*	*0.74 (1 – 20% T, 100% F)*
P9	*Integral 7.47 – 9.62 ps*	*0.83 (41 – 60% T, 100% F)*
P10	*Emax (maximum amplitude)*	*0.73 (81 – 100% T, 100% F)*
P11	*Power in spectrum at frequency = 1.11 THz*	*0.82 (61 – 80% T, 100% F)*

1. T = tumour, F = pure fibrous tissue or a mixture of fibrous and adipose tissue, 100% F = pure fibrous tissue only

Table 3: Performance of heuristic parameters with SVM classification, and wavelet deconvolution with Bayesian classification. SVM classification results are shown for individual parameters and parameter combinations that performed best in terms of accuracy. The best individual parameter and parameter combination is underlined.

Parameters	**Accuracy (%)**	**Sensitivity (%)**	**Specificity (%)**	**PPV[1] (%)**	**NPV[2] (%)**
P1	*73*	*87*	*62*	*65*	*85*
P2	*72*	*81*	*64*	*65*	*81*
P3	*70*	*77*	*65*	*64*	*78*
P4	*72*	*77*	*69*	*67*	*78*
P5	*72*	*92*	*56*	*63*	*90*
P6	*69*	*86*	*56*	*61*	*83*
P7	*69*	*87*	*54*	*61*	*84*
P8	*68*	*90*	*49*	*59*	*86*
P9	*56*	*69*	*46*	*51*	*64*
P10	*68*	*93*	*48*	*59*	*89*
P11	*56*	*56*	*57*	*51*	*61*
P1 and P6	*75*	*86*	*66*	*67*	*85*
P1, P6 and P11	*71*	*72*	*70*	*66*	*76*
P1, P6, P9 and P11	*67*	*56*	*75*	*65*	*68*
Gaussian wavelets	*69*	*87*	*54*	*60*	*84*

1. PPV = Positive predictive value
2. NPV = Negative predictive value